



# Analysis of the plasmonic power splitter and MUX/DEMUX suitable for photonic integrated circuits

Najmeh Nozhat, Nosrat Granpayeh\*

Faculty of Electrical and Computer Engineering, K. N. Toosi University of Technology, Tehran, Iran

## ARTICLE INFO

### Article history:

Received 1 December 2010

Received in revised form 29 January 2011

Accepted 1 March 2011

Available online 22 March 2011

### Keywords:

Surface plasmons  
Directional couplers  
Power splitters  
Multi/demultiplexers

## ABSTRACT

In this paper, the metal–insulator–metal (MIM) plasmonic directional coupler (PDC) with 45° waveguide bends based on surface plasmon polaritons (SPPs) excitation has been analyzed by the finite-difference time-domain (FDTD) numerical method. Effects of the variations of the coupler length and the metal gap thickness on the output powers and the propagation loss at 1550 nm wavelength have been studied. By choosing proper coupler lengths, power splitters with various output power ratios at 1550 nm wavelength and multi/demultiplexers, as some applications of the directional couplers have been proposed and their performances have been simulated.

© 2011 Elsevier B.V. All rights reserved.

## 1. Introduction

Miniaturizing the size, increasing the speed and improving the performance of the optical devices have attracted many researchers' attentions in recent years. However, due to the optical diffraction limit, there is a basic limit for minimization of the size of the conventional optical devices [1,2]. For this purpose, photonic crystals (PCs) are the key components for photonic integrated circuits (PICs), in which the lightwave guidance through sharp bends with very low loss is possible. These structures are periodic structures and need at least five periods to acquire photonic band gap. Therefore, the dimensions of the PC devices are in the order of light wavelength [1].

Surface plasmon polaritons (SPPs) are perfect candidates to overcome the diffraction limit and to propagate lightwave in the nanoscale devices and PICs. Surface plasmons are electromagnetic excitations that propagate through metal–dielectric interfaces. The SPP energy is confined very well over the surface and decay exponentially in the normal directions of both media [2–6].

There are various geometries for plasmonic waveguides, the major of which are insulator–metal–insulator (IMI) and metal–insulator–metal (MIM) structures. Insulator–metal–insulator structures can propagate waves in a long distance but their spatial extent, the distance between the points in two cladding layers where the field decays to 1/e of its peak value, is larger than the wavelength. Also, their light confinement is poor due to the dielectric cladding layers. Metal–

insulator–metal configurations are appropriate choices for application in the optical devices. The lightwave is guided in the dielectric core of MIM structure with high confinement. Furthermore, their spatial extent is in the order of subwavelength. Due to the higher losses created by metal claddings, the propagation length of MIM waveguides is lower; but it is enough for nanophotonic applications [1,6,7].

Several SPP-based nanophotonic structures and devices, such as metallic strips and nanowires [8], Bragg reflectors [9–12], plasmonic waveguides [13,14], filters [15], Mach–Zehnder interferometers [1,16], sensors [17], switches [18,19], wavelength sorters and beam splitters [1,2,20–22] have been proposed and analyzed, in recent decade. Also, the SPP power splitters have been fabricated and their experimental results have been shown [23–26].

In this paper, performance of the MIM plasmonic power splitters with various output power ratios at the wavelength of 1550 nm and multi/demultiplexers based on directional couplers has been analyzed and simulated by the FDTD numerical method. In Section 2, the simulation method and in Section 3, the results of the analysis and simulation of the plasmonic directional couplers (PDCs). Power splitters and multi/demultiplexers are described and discussed. The article is concluded in Section 4.

## 2. Analysis and simulation method

The finite-difference time-domain (FDTD) numerical method based on Yee algorithm, as a general and powerful algorithm for calculating the electromagnetic field distributions in structures with arbitrary geometry, has been employed for simulation of our proposed structures [27,28]. Since the simulation area is dispersive, the convolutional perfectly matched layer (CPML) has been used as the

\* Corresponding author. Tel.: +98 21 84062311; fax: +98 21 88462066.  
E-mail address: [granpayeh@eed.kntu.ac.ir](mailto:granpayeh@eed.kntu.ac.ir) (N. Granpayeh).

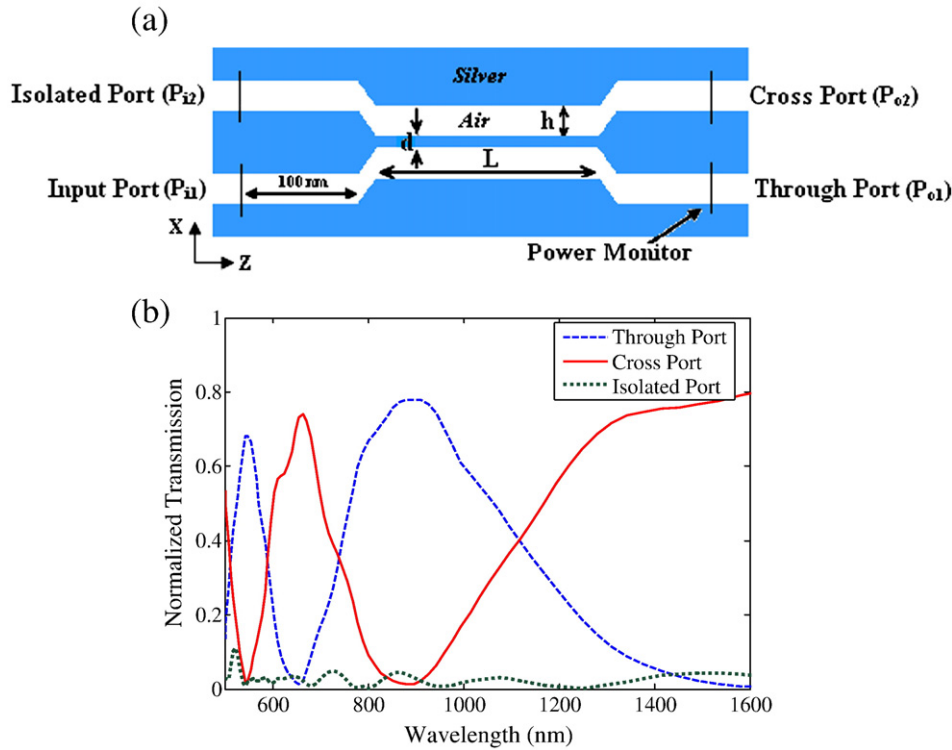


Fig. 1. The schematic view (a) and the normalized transmission spectra (b) of the plasmonic directional coupler with 45° bends.

absorbing boundary conditions [28]. The number of CPML layers is 11. The step size of the FDTD cell in  $x$  and  $z$  directions are  $\Delta x = \Delta z = 1$  nm and the time step is chosen by Courant condition to be  $\Delta t = 0.95 / \left( c\sqrt{(\Delta x)^{-2} + (\Delta z)^{-2}} \right)$ , where  $c$  is the free space speed of light. We have utilized MATLAB and C++ programming languages for our analyses and simulations. The time steps in our simulations are 60,000 and the dimensions of the simulation region are  $400\text{nm} \times 3000\text{nm}$ .

Since SPPs are excited by only TM polarization, a TM polarized pulse with electromagnetic field components of  $H_y$ ,  $E_x$  and  $E_z$  is launched to the MIM device, such as Fig. 1 [4,13].

The dispersion relation of SPP modes in two adjacent metal gap waveguides, with the guide width,  $h$  and metal gap thickness,  $d$ , has been obtained from the following equation [29,30]:

$$\frac{1-b}{1+b} = \pm e^{pd}, \quad (1)$$

with

$$b = \frac{[\epsilon_m k + \epsilon_d p - (\epsilon_m k - \epsilon_d p)e^{-2kh}] \epsilon_m k}{[\epsilon_m k + \epsilon_d p + (\epsilon_m k - \epsilon_d p)e^{-2kh}] \epsilon_d p}, \quad (2)$$

where  $k = \sqrt{\beta^2 - k_0^2 \epsilon_d}$  and  $p = \sqrt{\beta^2 - k_0^2 \epsilon_m}$  are the transverse propagation constants of the SPPs in dielectric and metal layers with relative permittivities of  $\epsilon_d$  and  $\epsilon_m$ , respectively.  $k_0 = 2\pi/\lambda$  is the free space wave number of the lightwave, where  $\lambda$  is the free space wavelength. The positive and negative signs in Eq. (1) are related to the symmetric and antisymmetric SPP modes in the waveguide, respectively. The propagation constant of SPPs can be defined as  $\beta = (\beta_s + \beta_a)/2$  [29,30], where  $\beta_s$  and  $\beta_a$  are the symmetric and antisymmetric propagation constants.

The coupling region has a major effect on the switching performance of the directional coupler. The coupling length,  $L_c$ , is the distance over which the energy of SPP modes couples completely

from one waveguide to the adjacent one, which depends on the difference between the propagation constants,  $\beta_s$  and  $\beta_a$  [2,30]:

$$L_c = \frac{\pi}{C} \left( m + \frac{1}{2} \right), \quad m = 0, 1, 2, \dots \quad (3)$$

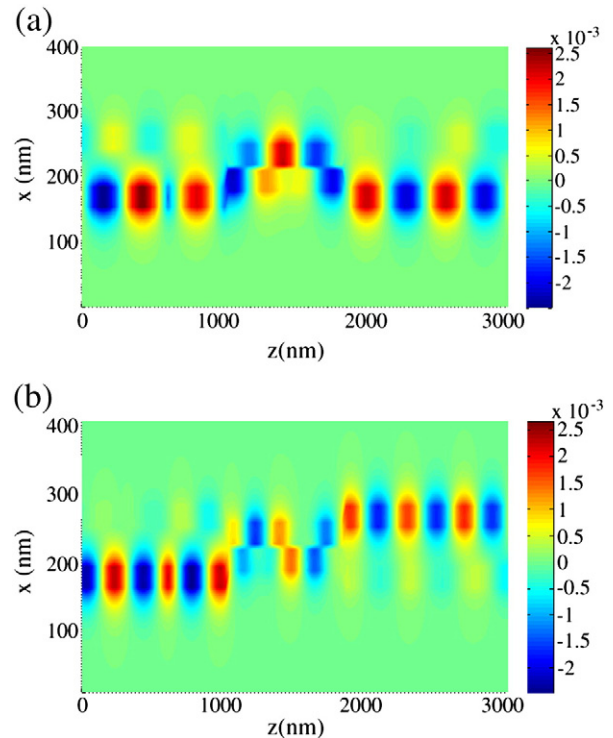
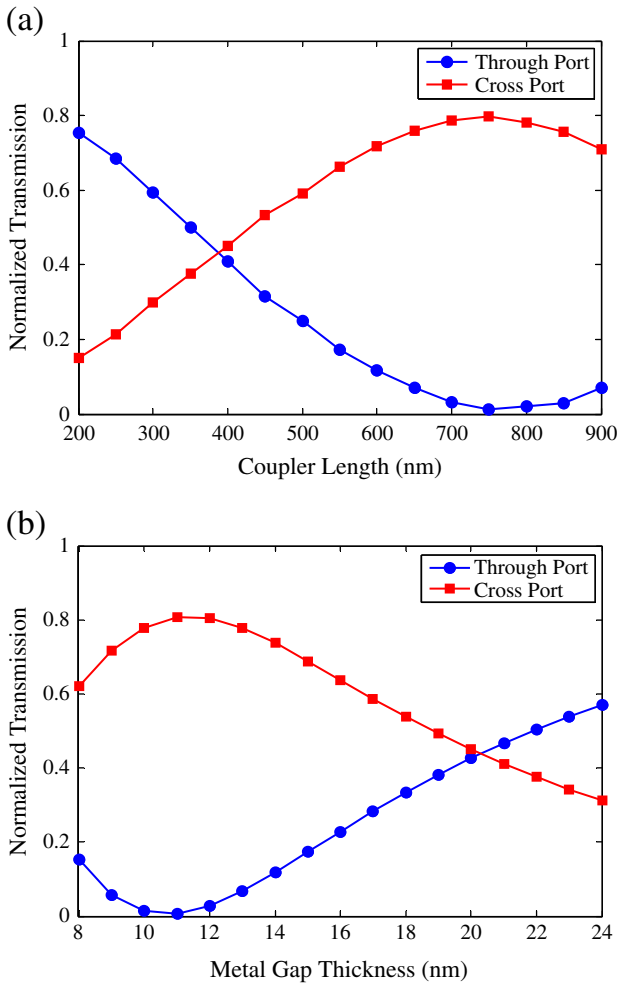


Fig. 2. Distributions of the magnetic field,  $H_y$ , of the directional coupler of Fig. 1 with  $h = 30$  nm,  $d = 10$  nm and  $L = 800$  nm at incident light wavelengths of (a)  $\lambda = 881$  nm and (b)  $\lambda = 655.4$  nm.



**Fig. 3.** Output powers versus (a) the coupler length for  $d = 10$  nm and (b) the metal gap thickness for  $L = 800$  nm at  $\lambda = 1550$  nm.

where  $C = (\beta_s - \beta_a)/2$  is the coupling coefficient. When the coupler length,  $L$ , is an odd multiple of the coupling length,  $L_c$ , the SPPs couple their whole energy from incident waveguide to the adjacent one and exit from it. On the other hand, when  $L$  is an even multiple of  $L_c$ , the lightwave exits from the incident waveguide [2].

We have solved the dispersion relation of Eq. (1) and obtained the propagation constant and the coupling length of SPPs. By increasing the metal gap thickness, the difference between the symmetric and antisymmetric propagation constants decreases. Therefore, for a constant coupler length, according to Eq. (3), the coupling length increases.

**3. Numerical results and discussions**

For analysis and simulation of proposed plasmonic power splitter and multi/demultiplexer based on the directional coupler, first, we have simulated the directional coupler of Fig. 1(a) with 45° bends. The thicknesses of the dielectric and the metal layers are chosen to be  $h = 30$  nm and  $d = 10$  nm, respectively. The length of the coupler is  $L = 800$  nm. Dielectric and metal layers are air and silver, respectively. The frequency dependent dielectric constant of the silver is expressed by the Drude model, which is acceptable in the frequency range of our simulation [3,31]:

$$\epsilon(\omega) = \epsilon_\infty - \frac{\omega_p^2}{\omega^2 - j\gamma_p\omega}, \tag{4}$$

where  $\epsilon_\infty$  is the relative permittivity at infinite frequency,  $\omega_p$  and  $\gamma_p$  are the plasma and collision angular frequencies, respectively. In this paper, the Drude parameters of silver are chosen to be  $\omega_p = 1.38 \times 10^{16}$  Hz,  $\gamma_p = 2.73 \times 10^{13}$  Hz and  $\epsilon_\infty = 3.7$  [31].

Illumination of the structure by a Gaussian modulated pulse results in the excitation of the SPPs at some wavelengths and there are some peaks at the outputs, as demonstrated in Fig. 1(b). The normalized power transmission is the ratios of the output powers to the input power. The maximum transmissions for the through and the cross ports occur at 881 nm and 655.4 nm wavelengths, respectively. As shown, the power at the isolated port is very low at these wavelengths.

Distributions of the magnetic field,  $H_y$ , at the above SPPs resonant wavelengths are depicted in Fig. 2. The lightwave exits from the through and the cross ports at 881 nm and 655.4 nm, after two and three times coupling, respectively. Therefore, the coupling lengths of the coupler for these two wavelengths are approximately 400 nm and 267 nm, respectively, whereas the coupling lengths obtained by Eq. (3) for 881 nm and 655.4 nm wavelengths are 437 nm and 284 nm, respectively. The differences between numerical and analytical results are due to the bends of the structure, since the coupling length in the theoretical method has been obtained from the dispersion relation of two adjacent straight waveguides.

The coupled wavelengths to the output ports are shifted by variation of the coupler parameters. For example, by increasing the coupler length, the coupled wavelength to the cross port,  $P_{o2}$ , increases, whereas by increasing the metal gap thickness,  $d$ , the wavelength decreases.

The output powers at through and cross ports in different coupler lengths,  $L$ , for  $d = 10$  nm and metal gap thicknesses,  $d$ , for  $L = 800$  nm at 1550 nm, the wavelength of the third telecommunication window, have been obtained and plotted in Fig. 3. By changing  $L$  and  $d$ , the

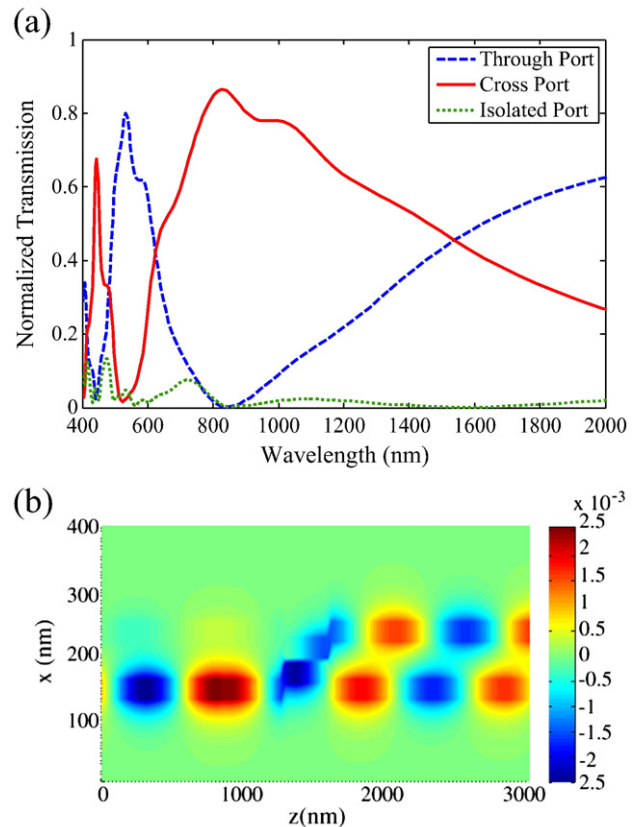


**Fig. 4.** Normalized transmission spectra (a) and the magnetic field distribution (b) of the directional coupler as a 3 dB power splitter for  $L = 350$  nm and  $d = 10$  nm.

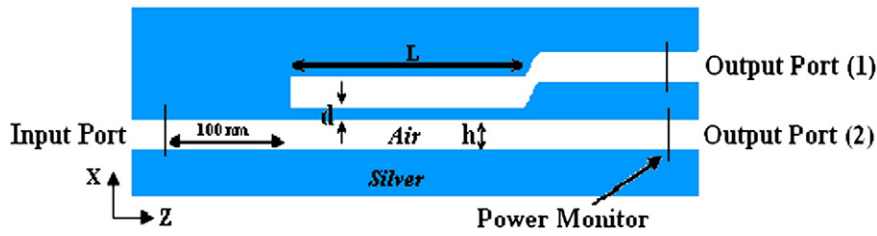


Fig. 5. Schematic view of a 10 dB power splitter with  $L = 600$  nm,  $h = 30$  nm, and  $d = 10$  nm.

input power couples periodically between output ports. As mentioned before, by increasing the metal gap thickness, the difference between  $\beta_a$  and  $\beta_s$  decreases, hence for a constant coupler length, according to Eq. (3), the coupling length increases, and the amount of power coupled to the cross port decreases. As shown in Fig. 3(b), the amount of power coupled to the cross port increases by increasing the gap thickness and since the coupling length for the gap thickness of  $d = 11$  nm at 1550 nm wavelength is 800 nm, the power is maximum for  $d = 11$  nm at the cross port. By further increasing the gap thickness, the power at cross port decreases and the power is exchanged between the output ports.

One of the most important factors in the performance of the directional couplers is the excess loss which is defined by  $-10\log\left(\sum_{j=1}^2 P_{oj} / P_{i1}\right)$ . We have investigated the excess loss of the PDC by variation of the coupler length and metal gap thickness. As we expect, the loss increases by increasing the coupler length. On the

other hand, by increasing the metal gap thickness, as it approaches the skin depth of the silver at the light wavelength of 1550 nm, the coupling to the cross waveguide is diminished, and the input lightwave transmits in the through port. Therefore, the coupler acts as a single waveguide and the interaction of lightwave and metal and hence the loss of the structure decreases.

### 3.1. Plasmonic power splitter

The proposed directional coupler can operate as a power splitter with various output power ratios for some special wavelengths. From Fig. 3(a), we can choose appropriate coupler length to obtain power dividers with different output power ratios. When the metal gap thickness is  $d = 10$  nm, the coupling length for 1550 nm wavelength is approximately 750 nm and the cross port power is maximum. For the coupler lengths less than 750 nm, the cross port power is reduced. For instance, with  $L = 600$  nm and  $d = 10$  nm, the coupler operates as

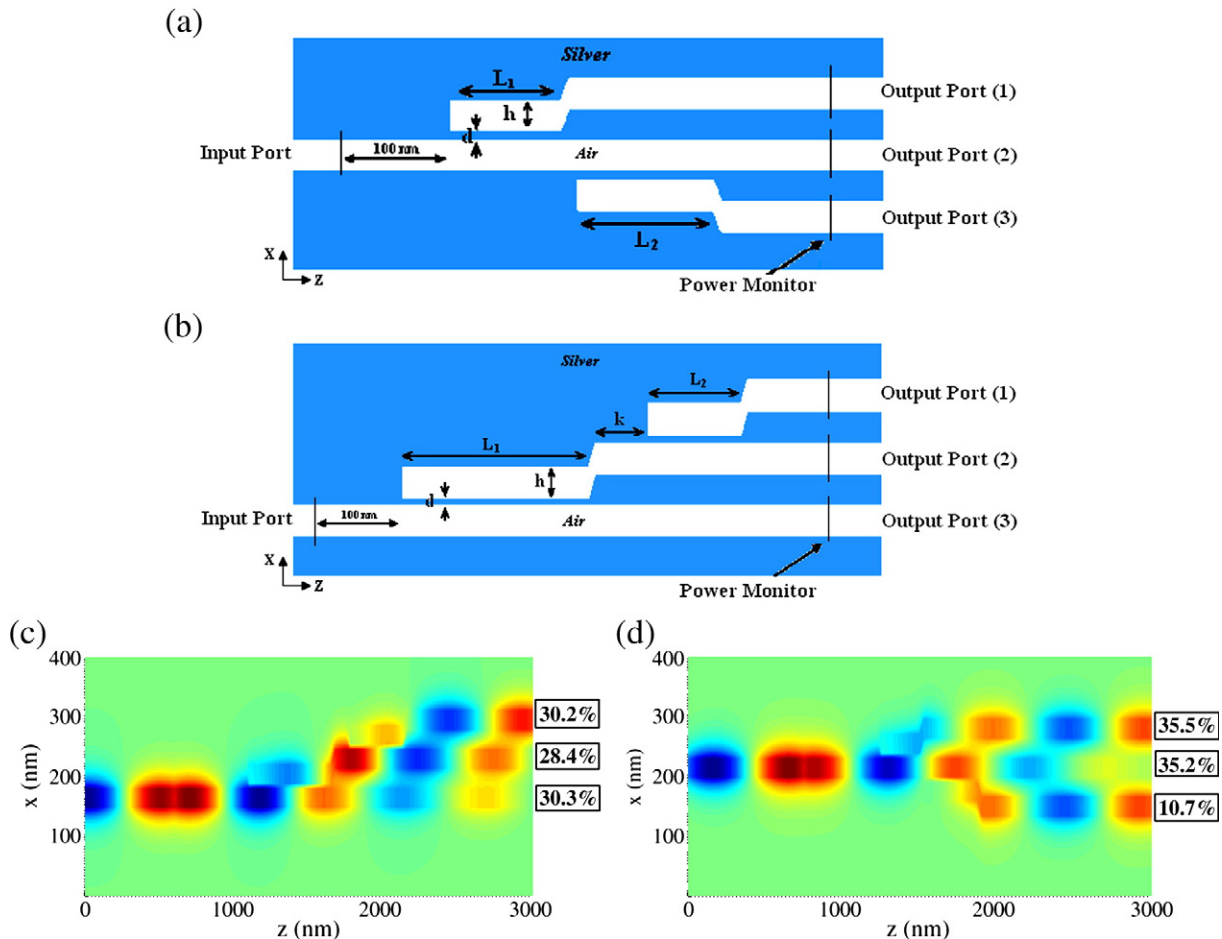
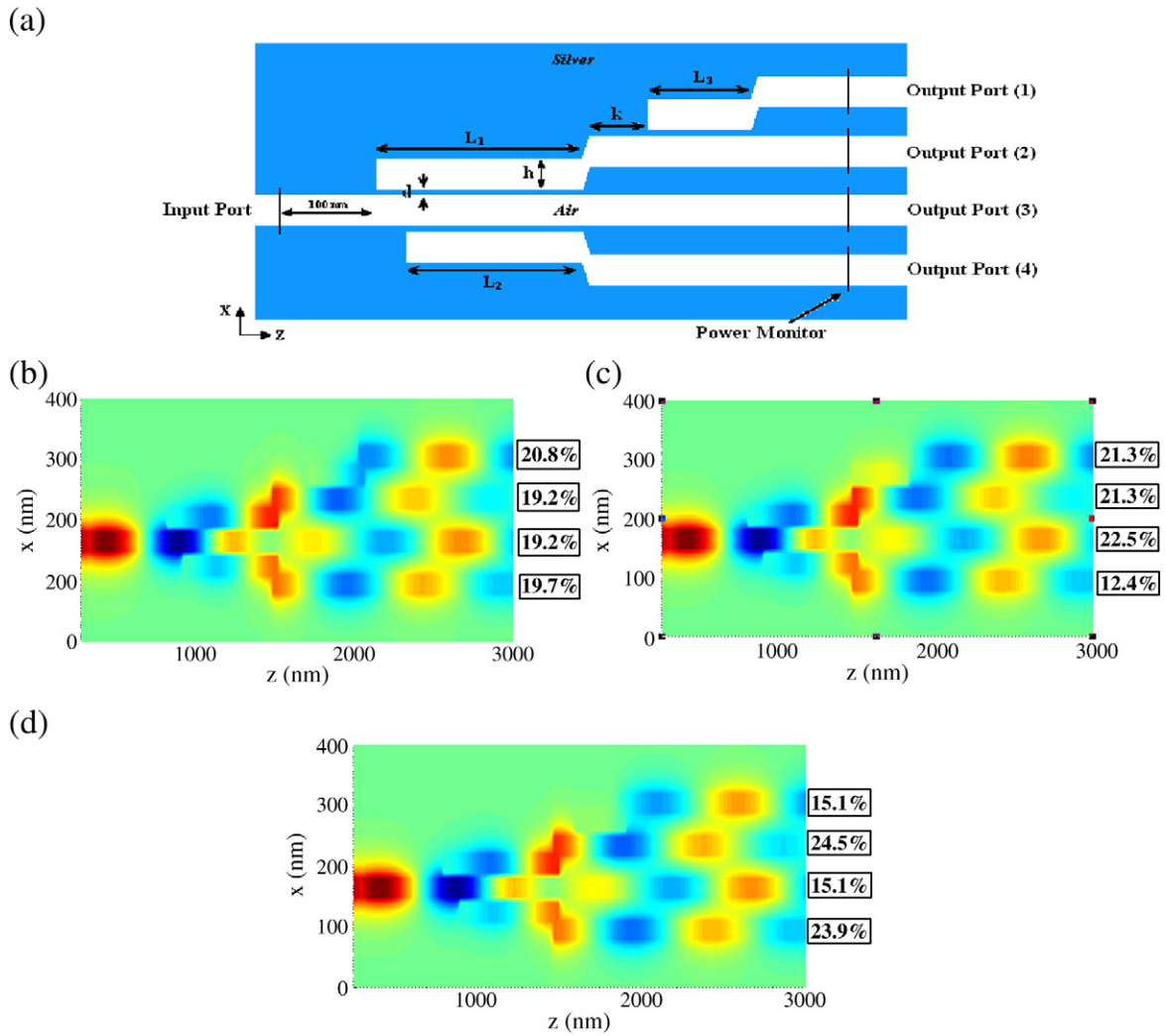


Fig. 6. (a) and (b) Schematic view of three output port power splitter. (c) and (d) Magnetic field distributions for various output power ratios. The parameters of the structure are  $L_1 = 250$  nm, and  $L_2 = 350$  nm for (c) and  $L_1 = 550$  nm,  $L_2 = 350$  nm, and  $k = 100$  nm for (d).



**Fig. 7.** (a) Schematic view of four output port power splitters. (b), (c) and (d) Magnetic field distributions for various output power ratios. The parameters of the structure are  $L_1=700$  nm,  $L_2=600$  nm,  $L_3=350$  nm, and  $k=200$  nm for (b),  $L_1=700$  nm,  $L_2=600$  nm,  $L_3=350$  nm, and  $k=0$  for (c), and  $L_1=700$  nm,  $L_2=600$  nm,  $L_3=300$  nm, and  $k=100$  nm for (d).

a 10 dB power splitter at  $\lambda = 1550$  nm, which the amount of power at through and cross ports are 9.9% and 76.5%, respectively. In order to obtain a 3 dB power splitter at wavelength of 1550 nm,  $L = 350$  nm, which the value of power at output ports will be 45.5%. The normalized transmission spectra and the magnetic field distribution of the 3 dB power splitter are depicted in Fig. 4.

A new proposed configuration for power splitter is illustrated in Fig. 5. From Fig. 3(a), we can determine the appropriate length for a 10 dB power splitter at 1550 nm wavelength to be  $L = 600$  nm. Then the output power at ports (1) and (2) are 77.2% and 10.4%, respectively.

The optical power can be divided to more outputs by increasing the proposed splitter branches. Three and four output power splitters and their magnetic field distributions are demonstrated in Figs. 6 and 7. The desired output power ratios can be derived by selecting the appropriate coupler branch lengths from Fig. 3(a).

### 3.2. Plasmonic multi/demultiplexer

Wavelength multiplexers (MUXs) and demultiplexers (DEMUXs) are essential components in wavelength division multiplexing

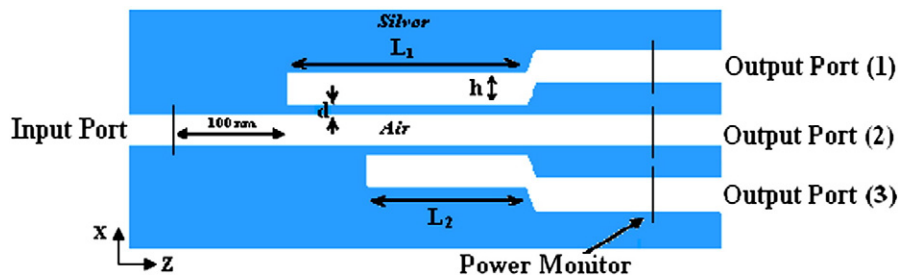


**Fig. 8.** Schematic view of a 3-channel multi/demultiplexer based on plasmonic directional couplers.

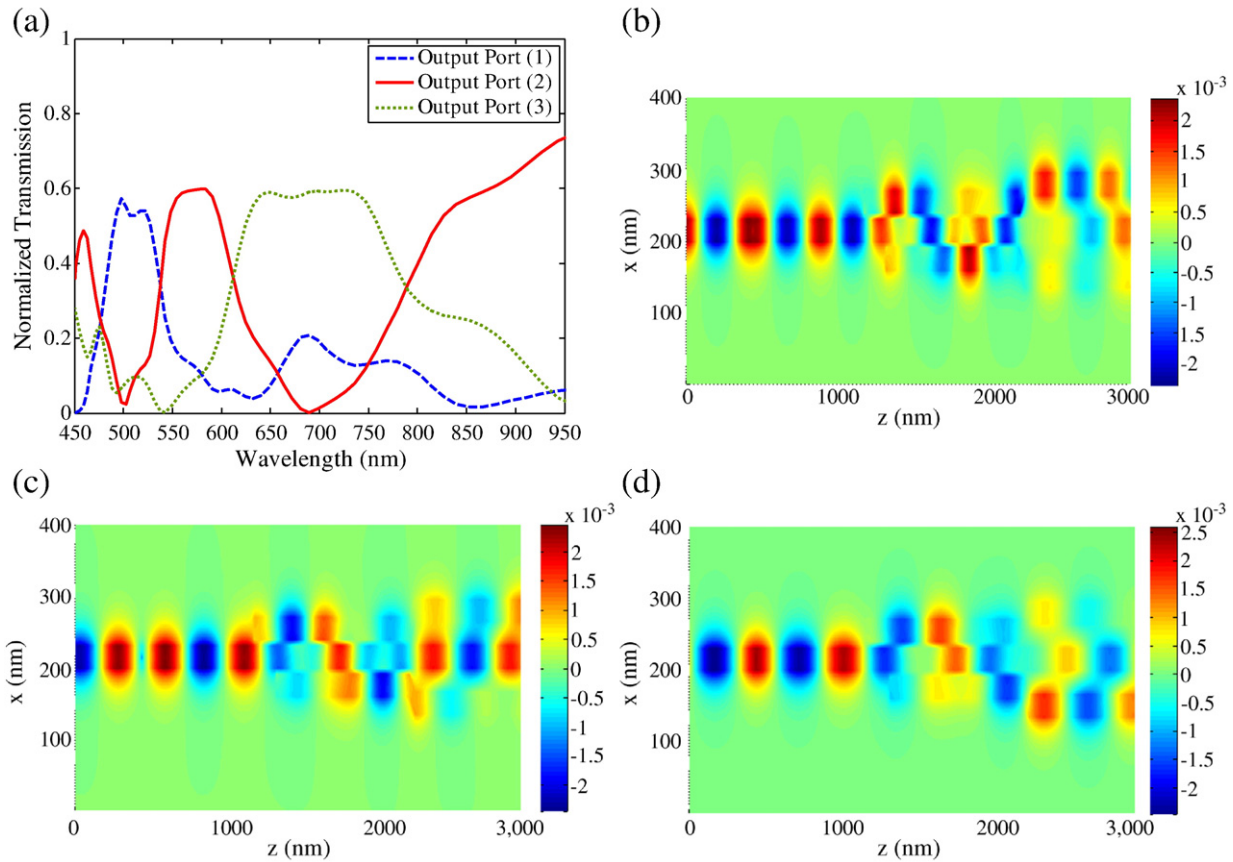


**Fig. 9.** (a) Normalized transmission spectra and magnetic field distributions to show the multiplexing performance of the three-channel multi/demultiplexer of Fig. 8 at wavelengths of (b)  $\lambda_1 = 502.2$  nm, (c)  $\lambda_2 = 577.9$  nm, and (d)  $\lambda_3 = 653.6$  nm.

(WDM) systems and bidirectional communication networks [32]. Wavelength selective multi/demultiplexers are divided into two groups of diffraction-based and interference-based schemes. For the first type diffraction gratings and for the latter, the optical fibers or the directional couplers can be employed. Therefore, another application of our proposed plasmonic directional coupler is the design and implementation of the nanoscale multi/demultiplexer. For multi/demultiplexing of  $N$  channels,  $(N-1)$  branches are required. Here, we have simulated a three-channel MUX/DEMUX.

For three-channel multi/demultiplexer, we have proposed the structure of Fig. 8 with two directional couplers of  $45^\circ$  waveguide bends. The lengths of the couplers are  $L_1 = 700$  nm and  $L_2 = 600$  nm. By exciting the structure with a Gaussian modulated pulse, three lightwaves with equi-spaced wavelengths of  $\lambda_1 = 502.2$  nm,  $\lambda_2 = 577.9$  nm, and  $\lambda_3 = 653.6$  nm exit at output ports 1, 2, and 3, respectively.

The normalized transmission spectra and the magnetic field distributions to show the demultiplexing performance of the three-channel multi/demultiplexer for the above mentioned wavelengths are demonstrated in Fig. 9. The three wavelengths of the input WDM lightwave are coupled to the relevant output ports of the device.

In multiplexing status, three lightwaves with equi-spaced wavelengths of  $\lambda_1$ ,  $\lambda_2$  and  $\lambda_3$  obtained in the previous stage, are simultaneously launched to the output ports, which are coupled and multiplexed to the input port, as shown in the transmission spectrum and magnetic field distribution of Fig. 10.

For simulation of our proposed power splitters and multi/demultiplexers, in order to have specific amount of power at output ports, at first we have chosen the coupler length from Fig. 3(a). But since the numerical FDTD method has some approximations, the obtained results do not exactly match with our prediction from

Fig. 3(a) and we saw very small changes. So, at the next stage, we have changed the coupler length and or the metal gap thickness in order to obtain the desired output powers.

In this paper, the plasmonic power splitters and multi/demultiplexers are formed by one, two and three waveguide branches. By utilizing more branches, the number of output ports can be expanded to develop the multi output ports power dividers or multi/demultiplexers.

#### 4. Conclusion

In this paper, plasmonic directional coupler with  $45^\circ$  waveguide bends have been analyzed and simulated by the FDTD method. Effects of the variation of the coupler length and the metal gap thickness on the performance of the directional coupler, at the wavelength of 1550 nm, have been studied. It has been shown that by increasing the gap thickness, the amount of power coupled to the cross port increases and it reaches to its maximum value for  $d = 11$  nm. By further increasing the metal gap thickness, as it approaches to the skin depth of silver at 1550 nm wavelength, the coupling to the cross waveguide is diminished, the coupler operates as a single waveguide and the interaction of lightwave and metal and hence the loss of the structure decreases.

The propagation losses of the directional coupler for different coupler lengths and metal gap thicknesses at the incident light wavelength of 1550 nm have been calculated.

From the spectrum of the output power of the directional coupler, we have proposed some devices, such as power splitters and multi/demultiplexers. By choosing appropriate coupler lengths, the performance of the plasmonic power splitters with various output power ratios at 1550 nm wavelength and multi/demultiplexers formed by

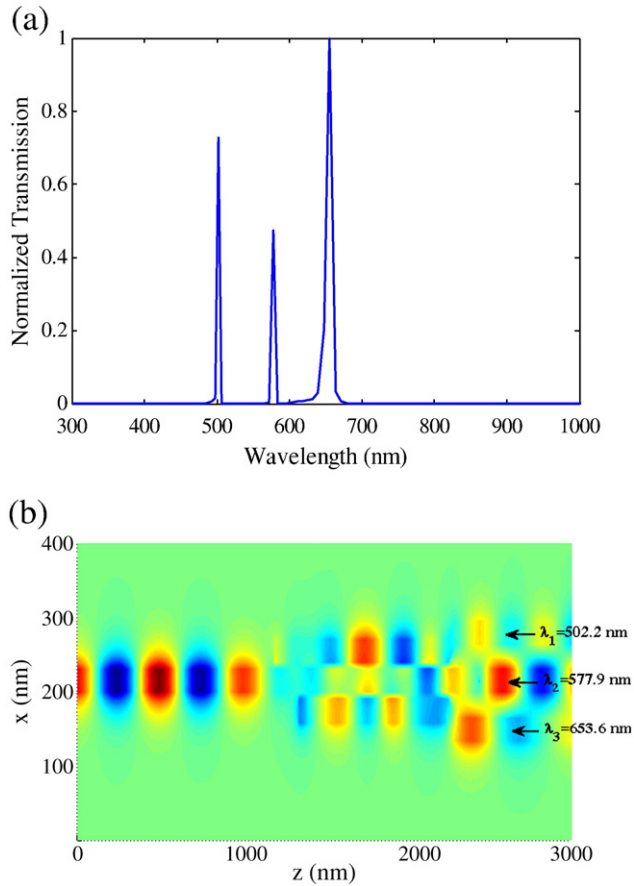


**Fig. 10.** (a) Normalized transmission spectrum and (b) magnetic field distribution of the device of Fig. 8 showing the multiplexing of three wavelengths of  $\lambda_1 = 502.2$  nm,  $\lambda_2 = 577.9$  nm, and  $\lambda_3 = 653.6$  nm.

one, two and three waveguide branches have been analyzed and simulated. By utilizing more branches, the multi output ports power dividers or multi/demultiplexers can be developed and their performances can be simulated by our prepared code.

## Acknowledgement

The authors would like to thank the Education and Research Institute for ICT (formerly, the Iran Telecommunication Research Center) for financial support of this project.

## References

- [1] Z. Han, L. Liu, E. Forsberg, *Opt. Commun.* 259 (2006) 690.
- [2] Z. Kang, G.P. Wang, *Opt. Express* 16 (2008) 7680.
- [3] H. Raether, *Surface Plasmons*, Springer, Berlin, 1988.
- [4] S.A. Maier, *Plasmonics: fundamentals and applications*, Springer, United Kingdom, 2007.
- [5] V.M. Shalaev, S. Kawata, *Nanophotonics with surface plasmons*, Elsevier, United Kingdom, 2007.
- [6] A. Hosseini, Y. Massoud, *Proc. of IEEE Conf. on Nanotechnol.*, Hong Kong, 2007, p. 81.
- [7] R. Zia, M.D. Selker, P.B. Catrysse, M.L. Brongersma, *J. Opt. Soc. Am. A* 21 (2004) 2442.
- [8] P. Berini, *J. Phys. Rev. B* 61 (2000) 10484.
- [9] B. Wang, G.P. Wang, *Appl. Phys. Lett.* 87 (2005) 013107-1-3.
- [10] H. Caglayan, I. Bulu, E. Ozbay, *Opt. Express* 13 (2005) 1666.
- [11] Z. Han, E. Forsberg, S. He, *IEEE Photon. Technol. Lett.* 19 (2007) 91.
- [12] J.Q. Liu, L.L. Wang, M.D. He, W.Q. Huang, D. Wang, B.S. Zou, S. Wen, *Opt. Express* 16 (2008) 4888.
- [13] A. Sellai, M. Elzaqin, *Phys. E* 41 (2008) 106.
- [14] B. Guo, G. Song, L. Chen, *Opt. Commun.* 281 (2008) 1123.
- [15] A. Hosseini, H. Nejati, Y. Massoud, *Opt. Express* 15 (2007) 15280.
- [16] L. Chen, B. Wang, G. Wang, *Appl. Phys. Lett.* 89 (2006) 243120-1-3.
- [17] G. Nemova, R. Kashap, *Opt. Commun.* 281 (2008) 1522.
- [18] M.L. Brongersma, J.W. Hartman, A. Atwater, *Phys. Rev. B* 62 (2000) R16356.
- [19] T. Nikolajsen, K. Leosson, S.I. Bozhevolnyi, *Appl. Phys. Lett.* 85 (2004) 5833.
- [20] C.Y. Tai, S.H. Chang, T. Chiu, *IEEE J. Photon. Technol. Lett.* 19 (2007) 1448.
- [21] Z. Han, S. He, *Opt. Commun.* 278 (2007) 199.
- [22] A. HuaWei, H. XuGuang, H. JingTang, *Sci. China Ser. G-Phys. Mech. Astron.* 51 (2008) 1877.
- [23] H. Ditlbacher, J.R. Krenn, G. Schider, A. Leitner, F.R. Aussenegg, *Appl. Phys. Lett.* 81 (2002) 1762.
- [24] J.R. Krenn, H. Ditlbacher, R.G. Schider, A. Hohenau, A. Leitner, F.R. Aussenegg, *J. Microsc.* 209 (2002) 167.
- [25] A.L. Stepanov, J.R. Krenn, H. Ditlbacher, A. Hohenau, A. Drezet, B. Steinberger, A. Leitner, F.R. Aussenegg, *Opt. Lett.* (2005) 1524.
- [26] A.B. Evlyukhin, S.I. Bozhevolnyi, A.L. Stepanov, J.R. Krenn, *Appl. Phys. B* 84 (2006) 29.
- [27] N. Nozhat, N. Granpayeh, *Progress in Electromagnetics Research, PIER* 99 (2009) 225.
- [28] A. Taflove, S.C. Hagness, *Computational electrodynamics: the finite-difference time-domain method*, Artech House, Boston, 2005.
- [29] X. Fan, G.P. Wang, J.C.W. Lee, C.T. Chan, *Phys. Rev. Lett.* 97 (2006) 073901-1-4.
- [30] Q. Zhu, D. Wang, J. Ye, Y. Zhang, *Opt. Commun.* 283 (2010) 1542.
- [31] J. Tao, X.G. Huang, X. Lin, Q. Zhang, X. Jin, *Opt. Express* 17 (2009) 13989.
- [32] G.P. Agrawal, *Fiber-optic communication systems*, John Wiley & Sons, Inc., New York, 2000.